



DEGREE PROJECT IN MEDICAL ENGINEERING,  
SECOND CYCLE, 60 CREDITS  
*STOCKHOLM, SWEDEN 2019*

# **Development of Ultrasound Pulse Sequences for Acoustic Droplet Vaporization**

Utveckling av ultraljudspulssekvenser för akustisk vaporisering av vätskedroppar

**ISABELLE GOUWY**

**KTH ROYAL INSTITUTE OF TECHNOLOGY  
SCHOOL OF ENGINEERING SCIENCES IN CHEMISTRY,  
BIOTECHNOLOGY AND HEALTH**



# Abstract

Ultrasound-mediated drug delivery has been proposed as a safe and non-invasive method to achieve localized drug release. Drug-loaded microbubbles are injected in the vascular system and ultrasound waves are then used to localize and burst the microbubbles at a specific targeted area. The relatively large size of microbubbles however limits both their lifetime and their reach in the human body.

Phase-change liquid droplets can extend the use of ultrasound contrast agents for localized drug delivery. Their smaller size provides several advantages. The droplets can reach smaller capillaries, such as those in tumors vasculature. Their lifetime is also considerably prolonged.

Through the phenomenon of Acoustic Droplet Vaporization (ADV), triggered by ultrasound stimulation, the liquid-filled droplets experience a phase change and are converted into gas-filled microbubbles. The newly created microbubbles can then be disrupted by further stimulation and release their drug load in the tumor tissue.

In this project, a protocol to image and burst perfluoropentane-based micro-sized droplets using a single transducer is developed using the Verasonics Ultrasound System. The pulse sequences are developed to allow close monitoring of the drug delivery by capturing a series of images before and after the vaporization or destruction of the droplets.

The droplets response was assessed for different pulse voltages and durations. Mean pixel value was calculated for the regions of interest, using the images captured before and after delivery of the ultrasound pulse.

Vaporization of the droplets can be achieved with low voltage (10V), whereas high voltage (50V) triggers their destruction.

Combined with high voltage, pulse duration affects the rate at which droplets can be destructed.

# Acknowledgements

First, I would like to express my gratitude to my supervisor, Associate Professor Dmitry Grishenkov, for his trust and valuable support on this project. His knowledge and guidance have motivated me not only throughout this thesis, but all along this Master's Programme.

I would also like to thank the students and researchers of the CEMIT Group, for their help and insightful input over these past months. I am particularly grateful to PhD students Hongjian Chen and Ksenia Loskutova for their considerate assistance and contributions.

Finally, special thanks to my partner, my parents and my friends for their continuous and unfailing support throughout my two years at KTH.

Isabelle Gouwy  
Stockholm, May 2019

# Table of contents

ABSTRACT	2
ACKNOWLEDGEMENTS	3
TABLE OF CONTENTS	4
LIST OF FIGURES	6
1. INTRODUCTION	7
2. MATERIALS AND METHODS	8
<b>2.1. Experimental setup</b>	<b>8</b>
2.1.1. Verasonics System	8
2.1.2. Transducer	9
2.1.3. Phantom	9
2.1.4. Droplets	10
<b>2.2. Data acquisition and processing</b>	<b>12</b>
<b>2.3. Image quality evaluation</b>	<b>14</b>
2.3.1. Regions of interest	14
2.3.2. Mean pixel value	14
<b>2.4. Ultrasound pulse techniques</b>	<b>15</b>
2.4.1. Imaging technique	15
2.4.2. Vaporization/Destruction technique	17
3. RESULTS	18
<b>3.1. Effects of imaging pulse</b>	<b>18</b>
<b>3.2. Effects of pulse duration</b>	<b>19</b>
<b>3.3. Effects of pulse voltage</b>	<b>20</b>
4. DISCUSSION	23
5. CONCLUSIONS AND FUTURE WORK	24
APPENDIX	25
<b>A.1. Ultrasound contrast agents</b>	<b>25</b>
1.1. Microbubbles	26

A.1.2. Oscillation modes	26
<b>A.2. Imaging techniques</b>	<b>28</b>
A.2.1. Conventional imaging	28
A.2.2. Contrast specific/Non-linear imaging	29
<b>A.3. Acoustic droplet vaporization</b>	<b>30</b>
A.3.1. Vaporization	31
A.3.2. Droplet structure and composition	32
A.3.3. Applications	32
<b>A.4. Limitations</b>	<b>33</b>
<b>REFERENCES</b>	<b>35</b>

# List of figures

Figure 1: Experimental setup composed of 1) Host computer, 2) Verasonics V-1 System, 3) Linear array transducer L7-4, 4) Tissue mimicking phantom, 5) Magnetic stirrer, 6) Droplet suspension and 7) Peristaltic pump. ....	8
Figure 2: L7-4 transducer from the Jonasson Centre for Medical Imaging. ....	9
Figure 3: Schematic representation of the tissue mimicking phantom's structure, adapted from [6]. ....	9
Figure 4: Preparation of the droplet emulsion: a) Addition of 0.5g of PFC5 and b) 18g of 0.28 wt% CNF suspension, c) mixed together. d) Sonication of the solution and e) creation of the droplet emulsion. ....	10
Figure 5: Droplet solution imaged before ultrasound exposure. ....	11
Figure 6: Size distribution at room temperature. ....	11
Figure 7: Droplet solution imaged after ultrasound exposure. ....	12
Figure 8: The Verasonics Sequence Object [9]. ....	13
Figure 9: The three ROIs selected for processing. ....	14
Figure 10: Pulse inversion longitudinal imaging of the vessel filled with droplet solution. ....	16
Figure 11: Equiripple bandpass filter around 6Mhz. ....	16
Figure 12: Mean pixel value in vessel ROI when imaging at different voltages. ....	18
Figure 13: Pulse Inversion Imaging at 50 V. ....	19
Figure 14: Mean pixel values of the three ROIs for 1-cycle (a), 8-cycles (b), 64-cycles (c) and 256-cycles (d). ....	19
Figure 15: Mean pixel values of the three ROIs for 10 V (a), 20 V (b), 30 V (c), 40 V (d) and 50 V (e). ....	21
Figure 16: Normalized mean pixel value for the ROI inside the vessel. ....	22
Figure 17: Microbubble changes in size with varying acoustic pressures [11]. ....	27
Figure 18: Microbubble response to increasing acoustic pressure [20]. ....	28
Figure 19: Illustration of the pulse inversion imaging technique [21]. ....	30
Figure 20: Illustration showing the extravasation of nanodroplets through endothelial cell gaps [2]. ....	31
Figure 21: Radius of an expanding bubble as a function of time and acoustic amplitude [3]. ....	32

# 1. Introduction

Ultrasound contrast agents have widely been used in ultrasonography to safely and effectively enhance the sensitivity and accuracy of the imaging technique. These contrast agents, most commonly gas filled micro-sized bubbles, significantly increase the intensity of the backscattered signal and thus allow visualization of otherwise invisible or difficult to image structures.

Microbubbles can also be used for therapeutic applications, in particular for targeted drug delivery. The ultrasound-triggered destruction of drug-loaded microbubbles allows localized release and deposition of the drug, which both increases the therapeutic index and decreases the risks of side effects [1].

There are however limitations to the use of microbubbles in such applications. Their relatively large size, in the order of several micrometers, prevents them from extravasating into tissue or to pass the lung capillaries. Also due to their size, microbubbles lifetime is only on the order of minutes once injected [2], considerably limiting treatment time.

Acoustic Droplet Vaporization (ADV), a phenomenon first described in the 1990s [2], could offer a solution to such issues. In ADV, the pressure of ultrasound waves causes liquid droplets to undergo a phase change and turn into gas-filled bubbles. Furthermore, in a way similar to regular microbubbles, sufficient acoustic pressure can cause the newly formed bubbles to cavitate and burst, thus releasing the drug they carry [3].

A specific application of ADV is the combination of diagnostic imaging, using the liquid droplets as ultrasound contrast agents to visualize the target site, together with therapy, using high intensity ultrasound to then disrupt these droplets and enable drug release at the target site. This combination is called theranostics [3]. With their smaller size, the droplets can reach narrower vasculature or even extravasate from the blood vessels and enter interstitial spaces such as the diseased interstitial space of tumors. Targeted drug delivery can then be achieved in extravascular targets [4].

For the droplets, using low solubility and low diffusivity liquids, such as perfluorocarbons, makes their lifetime significantly longer than that of microbubbles, ranging from a few days to a couple of months [2]. Additionally, and most importantly, perfluorocarbons are biocompatible and non-toxic [3].

In this thesis, an experimental protocol is developed to study perfluorocarbon core micro-sized droplets and the effect of different acoustic parameters on the droplets. Specifically, pulse sequences to both image and convert or burst the droplets are designed and tested using a commercially available transducer.

The sequences are developed to allow constant imaging of the target and to let the user trigger a “pre-burst images – burst – post-burst images” sequence on demand, using a single transducer for all operations.

The aim of this thesis is to assess the effect of the pulse sequences on the perfluorodroplets and consequently their ability to initiate ADV and droplet destruction.

## 2. Materials and methods

In the following chapter, a description of materials and instruments used for the experimental setup is provided. The ultrasound pulse sequences implemented to trigger the vaporization and destruction of the droplets, as well as the sequences used for imaging are also described.

### 2.1. Experimental setup

The experimental setup used for this project is presented in Figure 1.

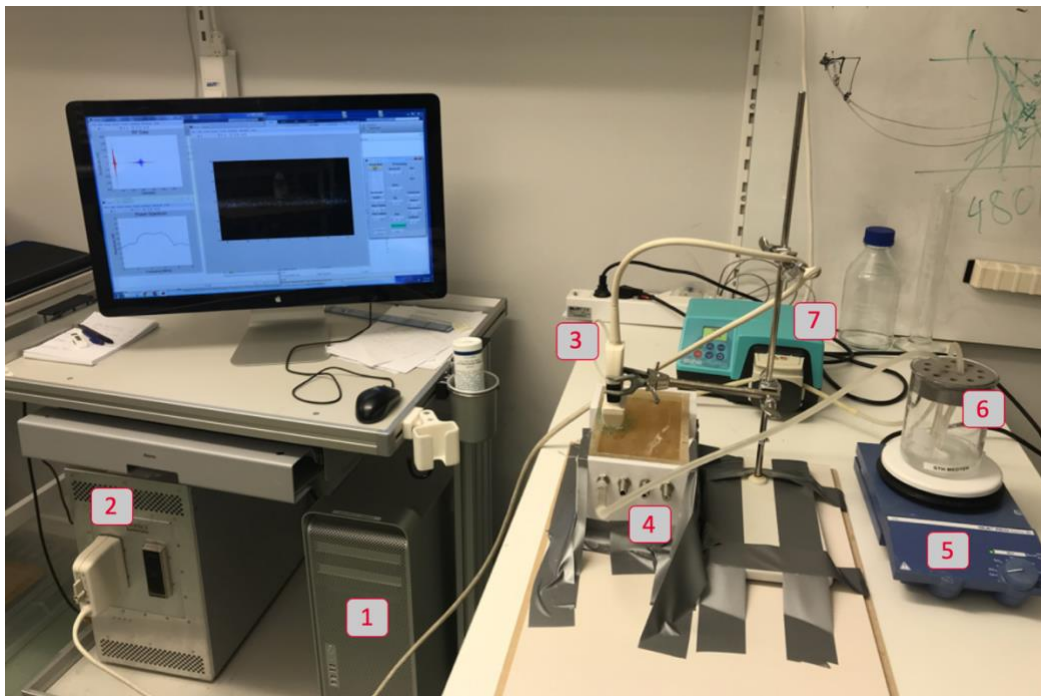


Figure 1: Experimental setup composed of 1) Host computer, 2) Verasonics V-1 System, 3) Linear array transducer L7-4, 4) Tissue mimicking phantom, 5) Magnetic stirrer, 6) Droplet suspension and 7) Peristaltic pump.

In the following sections, the main elements of this setup will be presented in more details.

#### 2.1.1. Verasonics System

The Verasonics V-1 System is a programmable ultrasound research tool. It can acquire, store, display and analyze data in a laboratory setting. The system includes the Verasonics Hardware and the Verasonics Software. The Verasonics Hardware consists of an acquisition module, with 256 transmit and 128 receive channels, each channel multiplexed to 1 of 2 transducer connectors. The Verasonics Software consists of the Verasonics Matlab Simulator, a hardware abstraction layers and other supporting tools.

Of greatest interest to us, the Verasonics Matlab Simulator uses the MATLAB environment to run ultrasound imaging sequences on the Verasonics Hardware [5].

One or two transducers can be connected to the Verasonics Hardware, that will then acquire, process and transfer the ultrasound signals from the transducer(s) to the host computer. The processed image is then rendered on the computer screen.

### 2.1.2. Transducer

The Philips ATL L7-4 is a linear array ultrasound transducer, with a frequency range of 4-7 MHz. It is composed of 128 elements and has a field of view of 38 mm.



Figure 2: L7-4 transducer from the Jonasson Centre for Medical Imaging.

The transducer in Figure 2 is the transducer used in our experimental setup and was connected to the scanhead connector of the Verasonics system. It is used both for imaging and to transmit the vaporization/destruction pulse sequences.

### 2.1.3. Phantom

The tissue mimicking phantom used for the experimental setup is the Peripheral Vascular Doppler Flow Phantom, Model 524, from ATS Laboratories.

It contains four simulated vessels of diameters 2, 4, 6 and 8 mm, located 15 mm below the scanning surface, as pictured in Figure 3.

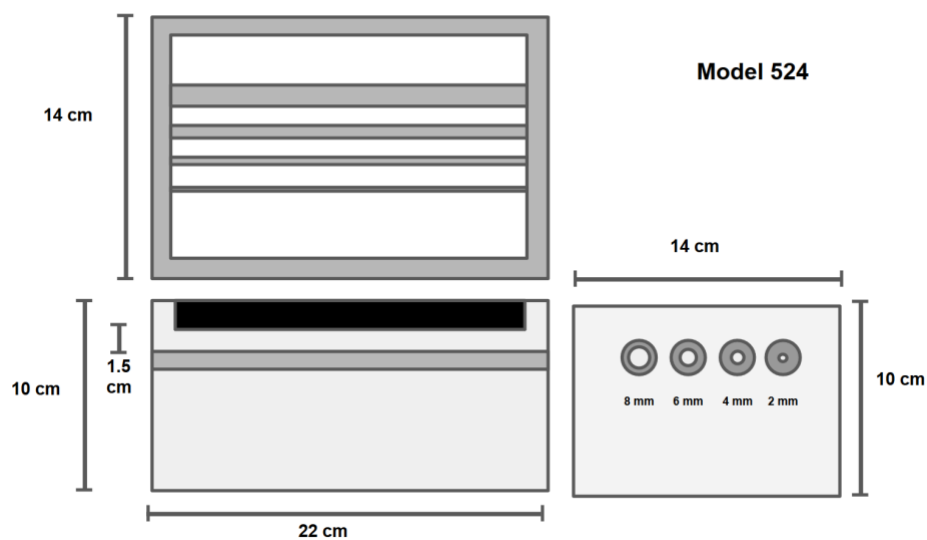


Figure 3: Schematic representation of the tissue mimicking phantom's structure, adapted from [6].

In the experimental setup, the 8mm vessel is filled with the droplet solution described in section 2.1.4.

For reference purposes during the preparation of the experiments, the 6mm wide vessel is filled with water.

#### 2.1.4. Droplets

##### *Fabrication*

The droplets used are perfluoropentane (PFC<sub>5</sub>) emulsion droplets stabilized by cationic cellulose nanofibers (CNF).

Droplet emulsions are formed when two immiscible liquids, such as oil and water, are mixed and droplets of one liquid is dispersed in the continuous phase of the other liquid [7].

In an oil-in-water emulsion, oil droplets are dispersed in the dispersion medium, water. Without stabilization, the droplets will however eventually coalesce. If solid particles are added to the emulsion, with the help of methods such as agitation or sonication, the particles will prevent droplet from coalescing by adsorbing into the oil-water interface and coating the individual droplets, thus stabilizing the interface [7].

The droplet emulsion used for the experimental setup was prepared as illustrated in Figure 4 and as follows.

The CNFs were produced using bleached sulfite pulp and had a dimension of about 3 to 5 nm in width, and about a few micrometers in length. A 0.28 wt% (weight percentage) CNF suspension was then obtained by dilution with Milli-Q water.

A mixture was then created by mixing 18 g of the CNF suspension to 0.5 g of perfluoropentane. The CNF-stabilized PFC<sub>5</sub> droplets were finally obtained by sonicating the mixture for about 1 minute at an amplitude of 80% using a Vibracell W750 (Sonics).

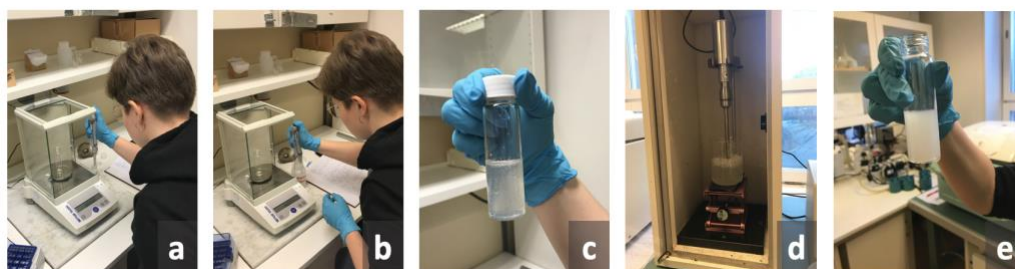


Figure 4: Preparation of the droplet emulsion: a) Addition of 0.5g of PFC<sub>5</sub> and b) 18g of 0.28 wt% CNF suspension, c) mixed together. d) Sonication of the solution and e) creation of the droplet emulsion.

The droplet emulsion used has a concentration of approximately 47 million droplets per milliliter. For the experiments, the emulsion is then diluted in Milli-Q water with a 1:10 dilution ratio.

##### *Microscopy tests*

A sample of the droplet solution is imaged with a 20X microscope, as seen in Figure 5, to measure the droplets initial size.

In average, the droplets are observed to be within the range of 1 to 5  $\mu\text{m}$ .



Figure 5: Droplet solution imaged before ultrasound exposure.

Additionally, the size distribution of the microdroplets was evaluated at room temperature in [8] and is represented in Figure 6.

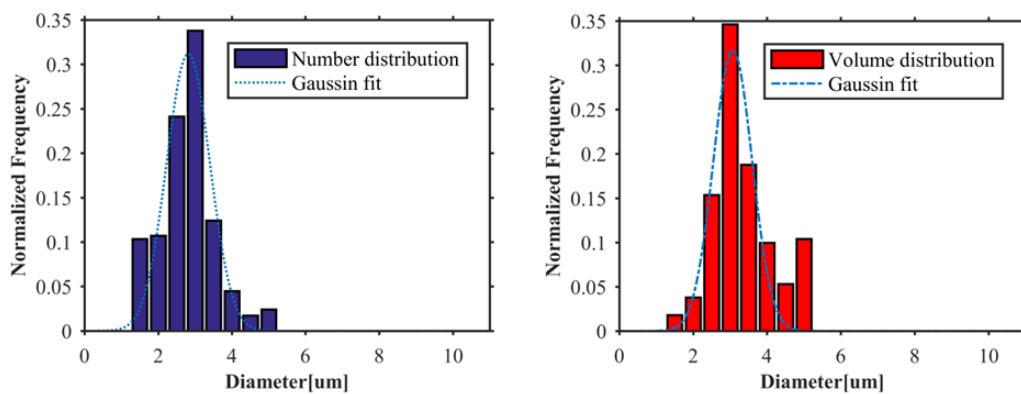


Figure 6: Size distribution at room temperature.

The sample is then exposed to an ultrasound pulse of varied amplitude and duration and imaged again to observe the formation of microbubbles and their size. A gas microbubble is observed in Figure 7, with a size of approximately 20 μm, around 8 times larger than an average-sized liquid droplet.



Figure 7: Droplet solution imaged after ultrasound exposure.

## 2.2. Data acquisition and processing

With the experimental setup in place, the L7-4 transducer is connected both for imaging purposes and for the droplet vaporization and destruction.

In order to observe and assess the vaporization and destruction mechanisms, images obtained with the transducer are captured before and after the ultrasound pulse, to study the ADV or destruction effect on the droplets. A sequence of events thus needs to be defined, specifying both the properties of the transmitted ultrasound pulses but also the ultrasound data to acquire and process.

As presented in Figure 8, a sequence is a list of events, which themselves contain a number of structures (or Objects) describing the different operations to be performed. These operations are executed sequentially but not all operations necessarily need to be defined for an event. The different operations permitted are: transmit, receive, reconstruct, process and control. These operation structures determine the actions carried out by the acquisition and processing systems of the Verasonics.

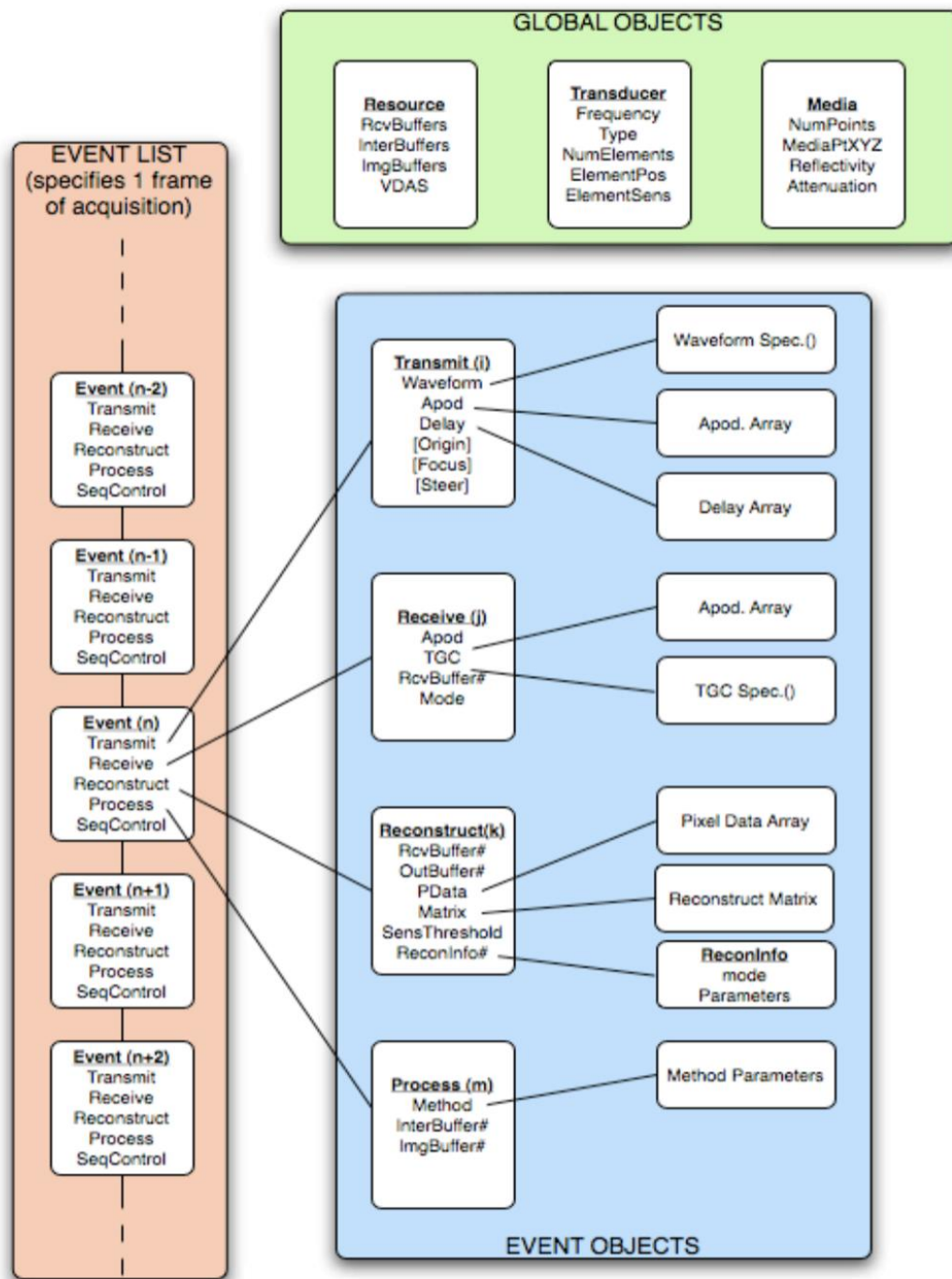


Figure 8: The Verasonics Sequence Object [9].

At the end of the sequence is a “jump back” event, which returns to the first event of the sequence. The sequence is then repeated indefinitely or until the user exits the program.

It is also possible to specify conditions to execute an event. When running our experiment, we don’t want to continuously transmit the vaporization or destruction pulses.

We then define our sequence object to continuously image with the transducer and add a user-activated trigger (presented to the user as a button on the user interface displayed on the screen) that will initiate the imaging-destruction-imaging sequence of events.

## 2.3. Image quality evaluation

### 2.3.1. Regions of interest

A region of interest (ROI) is a subset of the analyzed image. For each image obtained, three regions of interest of similar size were selected. Two of these regions were in the tissue part of the tissue mimicking phantom, while the third one was in the vessel containing the droplet solution

As shown in Figure 9, the ROI represented in green is in the tissue above the vessel, the ROI represented in red is centered inside the vessel, and the ROI represented in blue is in the tissue below the vessel. All three ROIs are vertically aligned.

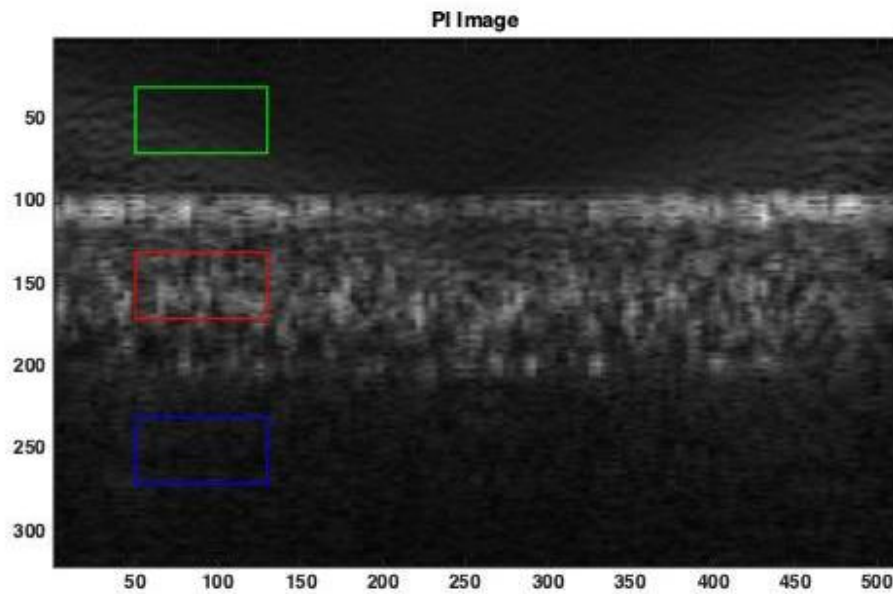


Figure 9: The three ROIs selected for processing.

### 2.3.2. Mean pixel value

For each region of interest, the intensity value of each individual pixel is added together and divided by the number of pixels in the ROI to obtain the mean pixel intensity. The value obtained is then in the range [0-255].

## 2.4. Ultrasound pulse techniques

As previously mentioned, the transmission of ultrasound pulses is performed by the Verasonics system, more specifically, the transmission of imaging pulses and the transmission of vaporization/destruction pulses.

For each of these transmit pulses, a number of characteristics need to be specified, which is done in the transmit operation of the corresponding event [5].

These include the transmit waveform, with its frequency, duration, duty cycle and polarity, the transmit power to use, but also which of the transducer elements are active and their timing.

In this experiment, imaging pulses are transmitted continuously with the L7-4 transducer, to obtain a longitudinal view of the phantom's 8mm vessel, filled with the droplet solution. A vaporization or a destruction pulse can also be transmitted on demand. The pulses are triggered by the user using the user interface on the screen.

### 2.4.1. Imaging technique

When using a transducer for imaging purposes, it is not enough to define a transmit operation it is also necessary to specify what to do with the data received after transmission of the pulse.

This is done in the receive operation of the event and allows for instance sampling and filtering of the received RF data [5].

By specifying the reconstruction and processing operations, an image can then be reconstructed from the RF data.

Using the L7-4 transducer and the two imaging techniques described below, an image is continuously displayed on the computer screen for the user.

When the user triggers a vaporization or a destruction pulse, the images acquired are also saved in a timestamped file. For each vaporization/destruction pulse delivered, 10 images, acquired with a time interval of 10ms are stored right before the payload delivery, and 10 images are acquired right after the delivery.

#### *B-mode*

Although the potential of ultrasound contrast agents is limited with fundamental B-mode imaging, the presence of contrast agents in a liquid increases the strength of the backscattered signal from this liquid and thus its echogenicity.

The imaging technique is thus used during the experiment as a reference to assess the added value and effectiveness of pulse inversion, a contrast specific imaging technique.

#### *Pulse inversion*

Pulse inversion is a technique in which non-linear components of the backscattered signal are isolated by subtracting the fundamental signal. In this technique, two consecutive pulses are transmitted, with the second pulse being 180° out of phase with the first one (meaning it is inverted). The received signals from the 2 pulses are then added together, and the linear components of each signal cancel each other out [1].

The remaining signal should then be composed of the echoes produced by the non-linear behavior of the contrast agents, as can be seen in Figure 10.

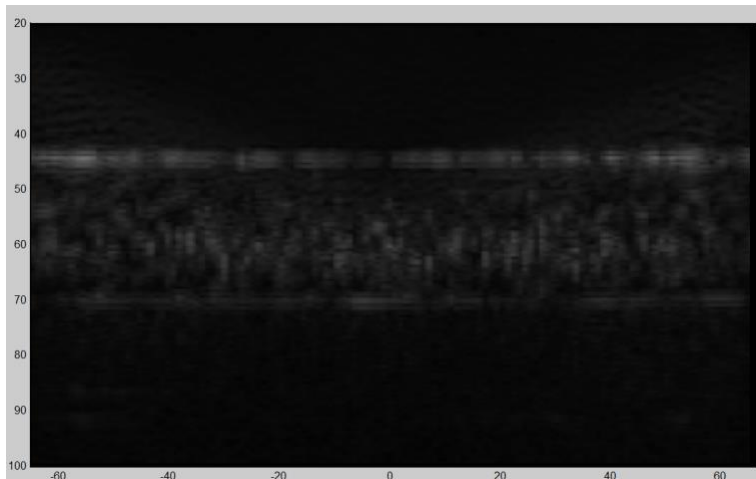


Figure 10: Pulse inversion longitudinal imaging of the vessel filled with droplet solution.

Additionally, to isolate the second harmonic components of the signal, an equiripple bandpass filter centered at twice the transmit frequency is implemented and used during the reconstruction of the signal.

The transducer used for the experiments has a frequency range of 4 to 7 MHz. Therefore, to keep both the transmit frequency and the second harmonic component as close as possible from the transducer's bandwidth, the chosen transmit frequency is 3 MHz, thus placing the second harmonic at 6 MHz. The magnitude response of the filter used when transmitting at the selected frequency is represented in Figure 11.

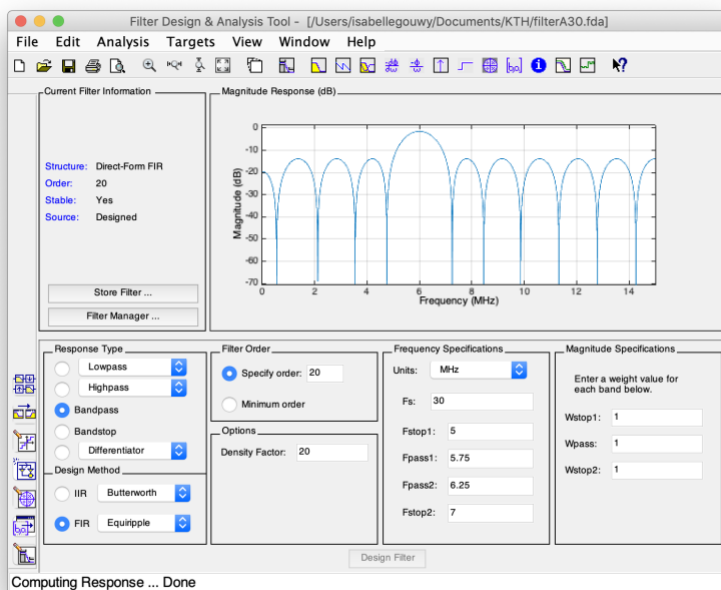


Figure 11: Equiripple bandpass filter around 6Mhz.

## 2.4.2 Vaporization/Destruction technique

To achieve acoustic droplet vaporization of the droplets, we are using a high-MI technique, meaning that we expose them to an acoustic field with a peak negative pressure high enough to favorize acoustic cavitation.

For each experiment run, the flow of droplet solution through the vessel is stopped, 10 high intensity pulses are consecutively triggered, with 10 images captured right before and right after the pulse delivery. The flow is then restarted, and 20 additional images are captured. Images are then analyzed and compared to evaluate the droplets response.

The high intensity pulse is developed using a special configuration of the Verasonics system. The configuration allows use of high transmit power levels with the “Extended Burst Option”. With this option, the system uses a dedicated power supply and can transmit bursts at power levels of up to 2000 Watts [9]. This value varies depending on the number of active elements transmitting, on the burst duration and on the load impedance.

For the experiments, all 128 elements of the transducer are activated and set to operate at full capacity, in order to maximize the volume of droplet solution that is insonated.

The frequency chosen for the pulse is 3.46 MHz, as we want the frequency to be relatively low to achieve high mechanical index, but also close from the transducer’s bandwidth. Other parameters are specifically set for each experiment. The transmit voltage has values ranging from 10 to 50V. The pulse duration is determined by the number of cycles in the transmit waveform. The number of cycles range from 1 to 384, which is the maximum achievable duration.

## 3. Results

In this section, we first assess the impact of the imaging pulse alone on the droplets. The efficiency of the high intensity pulse for vaporization and destruction of the droplets is then assessed, first based on the duration of the pulse, and next on the voltage of the pulse.

### 3.1. Effects of imaging pulse

For the first step of the experiments, we evaluate the imaging pulse alone. In particular, we assess the effect of the imaging voltage on the droplet solution.

After stopping the flow of droplets in the vessel, 10 images are captured at regular intervals over a period of 30 seconds. In Figure 12, the evolution of the mean pixel value inside the vessel is presented for each selected voltage.

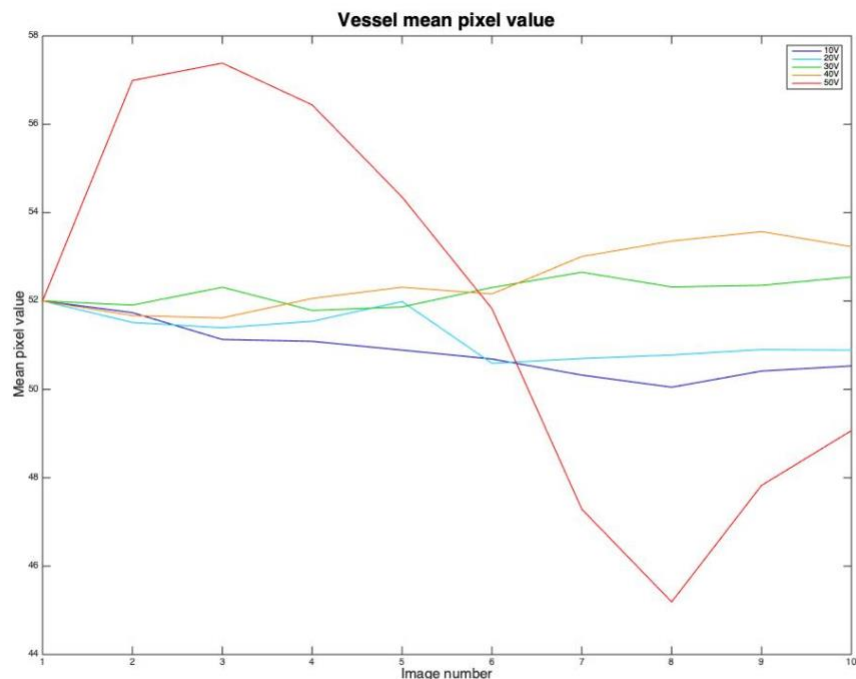


Figure 12: Mean pixel value in vessel ROI when imaging at different voltages.

At low imaging voltage (10 and 20 V), it is observed that there is only little variation of the mean pixel value in the vessel ROI, with a declining trend.

At slightly higher voltage (30 and 40 V), the variations are rather limited too, but with a tendency to increase.

In both cases, the range of variations is however only of about 1% of the maximum pixel intensity, it is thus small enough that it can be considered to be experimental errors.

With a voltage of 50 V, the effect of the imaging pulse on the droplets becomes noticeable. At first, the mean pixel value sharply increases to then drop to a value lower than the initial value. Such changes in intensity reflect a stronger backscattered signal from the region, consistent with the formation of gas microbubbles, followed by a decreasing signal, that would then be consistent with the destruction of the newly formed microbubbles.

Captures of the imaging at 50 V are coherent with this assumption. In Figure 13, consecutive frames show the formation of a microbubble, its ascension towards the top of

the vessel (despite the ultrasound radiation force pushing the droplets downwards) and finally its destruction.

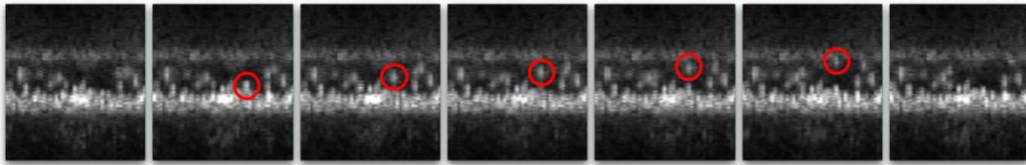


Figure 13: Pulse Inversion Imaging at 50 V.

### 3.2. Effects of pulse duration

In this series of experiments, the voltage used for the destructive pulse remains constant and maximal, at 50V. The pulse duration however varies, starting with 1 cycle, 8 cycles, 64 cycles and finally 256 cycles. The imaging voltage was 10 V.

The charts in Figure 14 represent the evolution of the mean pixel values for each ROI throughout the delivery of 10 consecutive pulses with the selected number of cycles. The dotted vertical lines labelled “P1” to “P10” mark when the destructive pulses were triggered. Similarly, the “Flow” line marks when the flow in the vessel was restored.

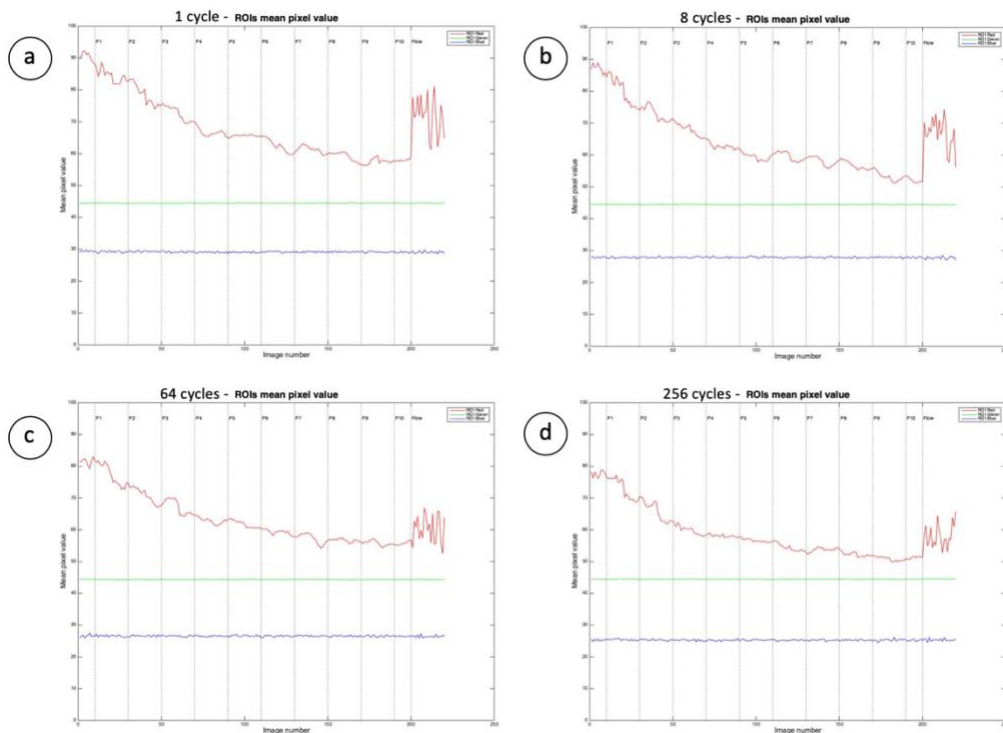


Figure 14: Mean pixel values of the three ROIs for 1-cycle (a), 8-cycles (b), 64-cycles (c) and 256-cycles (d).

In the first experiment, the pulse delivered is 1-cycle long. Overall, the mean pixel value in the vessel ROI (in red) decreases continuously, with a sharper decrease during the first six applied pulses.

After restoration on the flow, the intensity then suddenly increases, consistent with replenishment of the droplets in the area. Although the initial intensity value is not fully

restored after the 20 images captured for the experiment, the intensity spikes observed are progressively approaching that value.

For the second experiment, with 8 cycles, a similar behavior is observed. Up until the fifth pulse, the decrease in intensity is relatively steady and then continues at a slower rate for the remaining five pulses. The replenishment of droplets is also comparable, with a substantial increase of the mean pixel value after restoring the flow.

Next, the experiment is run with a pulse duration of 64 cycles. The decrease in pixel intensity here slows down earlier than in the previous tests. After delivery of the 4<sup>th</sup> pulse, the decrease rate is more gradual. It is worth noting that after restarting the flow, less droplets seem to recirculate in the system. One explanation for this is that the same sample is used for all the experiments run. It is therefore possible that destruction of the droplets in previous experiments has a negative impact on the droplet concentration.

This is also visible when comparing the intensity value at the beginning of this experiment with the previous experiments.

Finally, with 256 cycles, the sharper decrease in mean pixel value is only observed during delivery of the first three pulses. For the remaining 7 pulses, only a gradual decrease is observed. Compared with the previous experiment, the initial intensity value is lower and the droplet replenishment weaker, indicating an even lower droplet concentration.

### **3.3. Effects of pulse voltage**

For these experiments, maximum pulse duration is chosen, 384 cycles, and five different voltages are tested: 10 V, 20 V, 30 V, 40 V and 50 V. The imaging voltage was again 10 V. The evolution of the mean pixel values for each ROI is plotted in Figure 15 for each selected voltage.

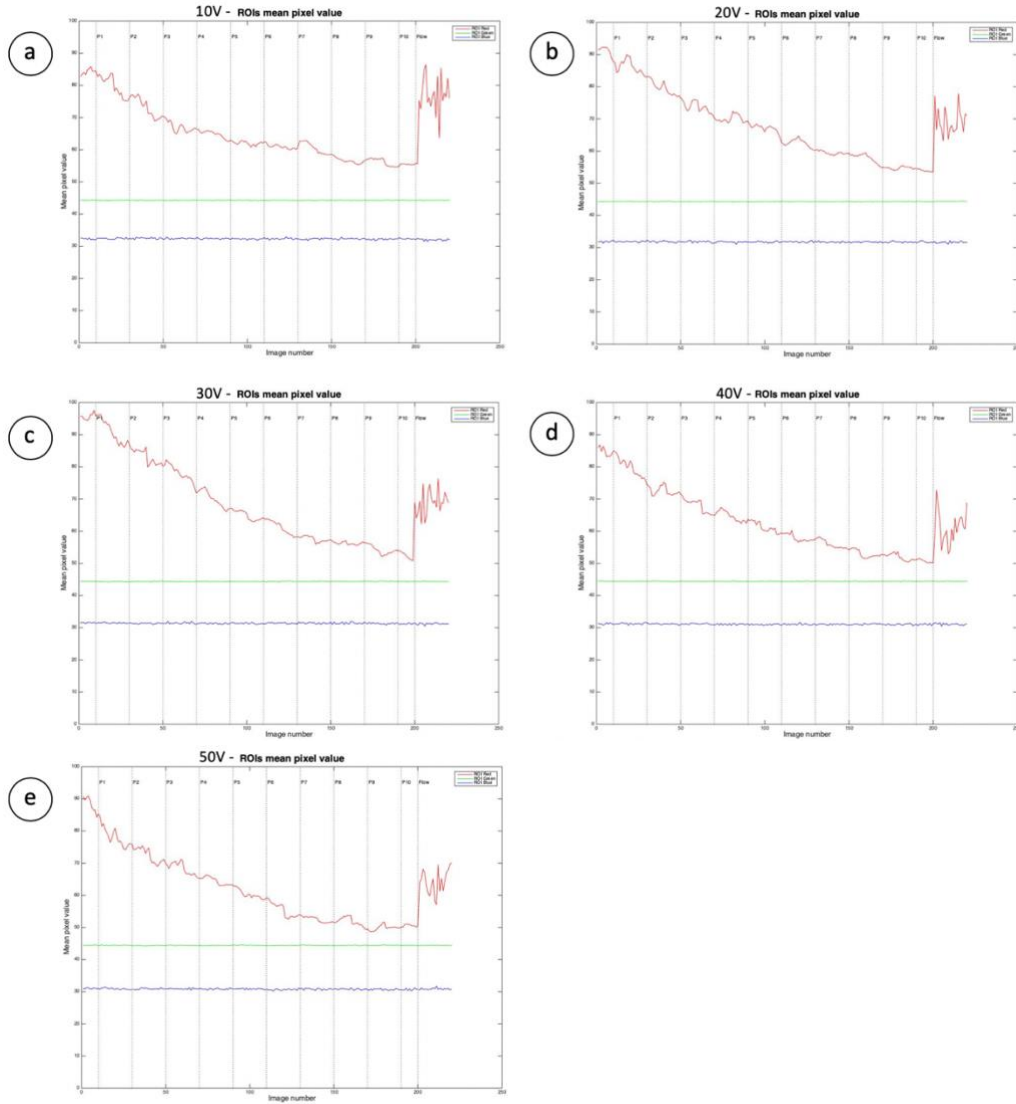


Figure 15: Mean pixel values of the three ROIs for 10 V (a), 20 V (b), 30 V (c), 40 V (d) and 50 V (e).

As a general observation, the mean pixel value of the region inside the vessel drops with every burst delivered, regardless of the voltage selected. As comparison points, we can observe that the mean pixel values of the two other regions, in the tissue, are relatively stable and constant. The decrease in mean pixel value is however noticeably faster with increasing voltage.

To more easily compare the effects of the different voltages, we first normalize the mean pixel values inside the vessel for each experiment and present the plots of these datasets in one figure, Figure 16.

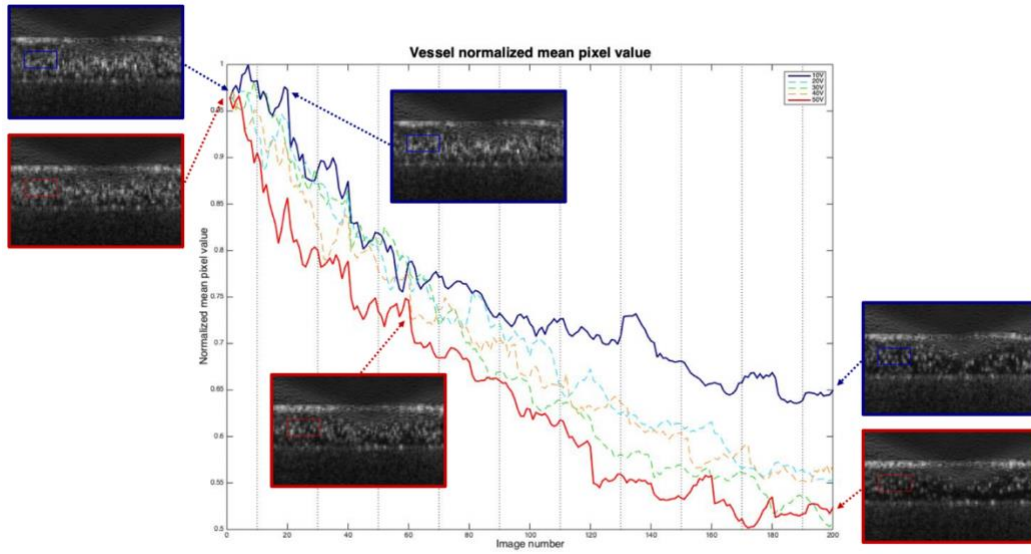


Figure 16: Normalized mean pixel value for the ROI inside the vessel

In particular, we focus on the most extreme voltages in both directions: 10 V and 50 V. At 10 V, after the 10 consecutive pulses, about a third of the initial intensity value is lost. After the first two pulses, intensity spikes higher than the value before the pulse delivery are visible. This increase in intensity indicates a stronger echo in the ROI, consistent with the formation of gas microbubbles. This is also observed after delivery of the 7<sup>th</sup> pulse.

At 50 V, these intensity spikes are mainly not present, except after delivery of the 3<sup>rd</sup> pulse. After the 10 pulses, about half of the initial intensity value is lost, indicating a more destructive behavior.

## 4. Discussion

Three sets of experiments were performed for this project.

The aim of the first set was to evaluate the possible impact of the imaging pulse on the droplets. This is important information because the imaging functionality should only serve for diagnostic purposes, to localize and visualize the contrast agents in the target area, and to monitor the ultrasound-mediated drug delivery.

As discussed in section 3.1, imaging with the maximum voltage (50 V) had a visibly destructive effect on the droplet, this voltage should then unquestionably not be used for imaging purposes.

Although the results obtained at lower voltages had such small variations that they can be attributed to experimental errors, with higher voltages (30 and 40 V), the mean pixel value of the ROI were gradually increasing. Since these experiments were only performed for a short duration of time, one could argue that this trend could become significantly increase after a prolonged ultrasound exposure. If it were to happen, this would mean that the imaging pulse would provide enough energy for the droplets to be converted into gas-filled microbubbles.

The experiments showed that with the pulse inversion technique, the droplets were visible and thus served as contrast agents even at the lowest voltage tested with. It is therefore sufficient to image with a voltage of 10 V, and thus avoid any undesirable effect on the droplets.

For the second set of experiment, the effects of the duration of the high intensity pulse was evaluated. It should first be mentioned that an aspect of the experimental setup seemed to have impacted the initial conditions of the experiments. Indeed, the same sample was used for all the experiments. In Figure 14, the results are presented in the order in which the experiments were run. One can easily notice that the initial value for the mean pixel intensity is increasingly lower for each new experiment. The voltage used for the high intensity pulse was 50 V, it is therefore likely that each new pulse delivered burst a certain amount of droplet.

The duration of the pulses applied had an impact on the rate at which the pixel intensity decreased. For shorter pulses, we observed a slower decline, whereas for long pulses, only after a couple of pulses, most of the effect on the droplet was achieved.

Finally, the last set of experiment was meant to test the impact of the high intensity pulse voltage.

At 10 V, results suggest that the pulse triggers a phase change of the droplets to gas, thus achieving ADV. In general, the mean pixel intensity of the ROI however decreases, either suggesting displacement of the gas microbubbles or their destruction.

At 50 V, a clear destructive behavior is displayed. The mean pixel intensity of the ROI drops by half and ADV is seemingly less susceptible to happen. The high intensity pulse, with high voltage and long duration, thus appears to burst the droplets.

## 5. Conclusions and Future Work

In the presented work, a protocol was developed to image and activate perfluoropentane droplets using a single linear array transducer. The design of a specific “image – burst – image” pulse sequence allowed consistent tracking of the effect of the burst pulse on the imaged area.

Results demonstrated that both the pulse duration and the pulse voltage had an impact on the activation of the droplets. Although a high voltage quite consistently showed destruction of the droplets, the pulse duration proportionally affected the rate of destruction.

On the other hand, a lower voltage showed a different effect on the droplets, enabling their vaporization.

With this protocol, the user can easily configure the pulse duration and voltage of the burst pulse, meaning they could potentially control real-time whether to vaporize the droplets into gas-filled microbubbles or to destroy them and release their content.

Additionally, selection of the voltage parameter for the pulse inversion imaging showed to have a destructive effect on the droplet if set too high. The voltage used for imaging should therefore carefully be chosen; although it should be kept as low as possible, a minimum voltage is needed to visualize the droplets as contrast agents. In our experiments, a voltage of 10 V proved to be sufficient and to show no effect in the droplets.

In the future, the protocol could be greatly improved by giving the user the ability to fully customize the pulse sequences delivered, allowing them to choose the number of high intensity pulses delivered in a row, at a specific time interval. Similarly, settings to select the number of images to be captured before and after the pulse delivery and their timing could be configurable via the user interface.

The pulse sequences could also be adapted to work with different transducers. The transducer used in this project, the L7-4, has a rather narrow bandwidth, and it could be interesting to test the protocol with a broader range of frequencies. By extending its possibilities of use, this protocol could be a valuable tool to evaluate the promises of liquid-filled droplets as theranostic agents.

# Appendix

Today, most common cancer therapies include surgery, chemotherapy and radiation therapy. These treatments however expose patients to adverse side effects, in particular, the non-negligible damages caused by ionizing radiations and chemotherapeutic drugs to healthy cells [10].

Therefore, great effort has been devoted in the past decades to improve the efficacy of cancer therapy in the region of the tumor, while reducing the undesirable side effects in healthy tissues [1]. This is the main goal of temporally and spatially controlled therapy and drug delivery, which uses a specific stimulus, internal or external, to trigger a process, such as drug release [2].

An example of internal stimulus used is acidity of the medium, or pH. However, most techniques use external stimuli, such as a magnetic field in targeted magnetic nanoparticle therapy, a neutron beam in boron neutron capture therapy, or light energy in photodynamic therapy [1]. Mechanical energy can also be used as an external stimulus, in particular in ultrasound therapy.

Ultrasound has many advantages over other mentioned techniques. It is relatively low cost, uses portable equipment and provides real-time images of the target area. Most importantly for therapeutic applications, it is also non-invasive and doesn't expose the patient to ionizing radiations [1].

As a diagnostic imaging modality, ultrasound already is the most widely used technique, and provides the ability to penetrate deep into the body and to easily focus on specific targets.

Based on the echoes generated by reflection or scattering of ultrasound waves at different tissue and structure boundaries, a cross sectional image representing these tissues and structures is generated. Although blood is difficult to image as it poorly scatters ultrasound signals, it has been demonstrated that the intravenous injection of gas-filled microbubbles in the bloodstream increases echogenicity of the blood [1]. If therapeutic agents are incorporated into these microbubbles, a therapeutic payload can potentially be released at a specific site. The spatially and temporally controlled release can be triggered by exposing the drug-loaded microbubbles [2]. This can be achieved under specific conditions and involves a number of mechanisms that will be presented in the following sections.

## A.1. Ultrasound contrast agents

Ultrasonic contrast agents are echo-enhancing agents used in medical ultrasound imaging to improve the contrast between different structures and thus increase the sensitivity of the imaging technique, and to visualize otherwise invisible structures [11]. There are two mechanisms by which ultrasonic contrast agents achieve contrast enhancement. First, these agents are, most often, gas-filled microbubbles and the high difference in acoustic impedance between the gas and the surrounding tissue means that a large portion of the ultrasound wave is scattered, and partly reflected back to the transducer.

The second mechanism is the oscillations undergone by the agent in response to the ultrasonic wave. These oscillations are possible due to the compressibility of the gas in the microbubble and are responsible for generating non-linear components in the acoustic response from the microbubble [11].

Ultrasound contrast agents have been used since the late 1960s and were then free air microbubbles that formed at the site of injection of a saline solution. Today, the commercially available agents are pharmaceutically developed with different methods allowing a strict control over their size, stability and structure [12].

## 1.1. Microbubbles

Microbubbles have a variety of properties that are of importance for their use as ultrasonic contrast agents. These include three main properties: their size, the composition of their shell and of the composition of their core (their gas content). As a direct result of these three properties, a set of other properties is derived. This includes persistence, fragility, resonance, attenuation, adhesion, safety, preparation or cost [13].

### *Size*

Although the majority of commercially available microbubbles range within 1-2  $\mu\text{m}$ , the overall available range of microbubbles is approximately between 1-20  $\mu\text{m}$  [14]. This wide range is a consequence of the methods used to fabricate them, such as sonication, in which sound energy is applied to a liquid containing particles.

Depending on their size, microbubbles have different properties. Their persistence in circulation is for instance proportional to their size, and larger microbubbles ( $> 4 \mu\text{m}$ ) persist longer than smaller ones [14].

Smaller microbubbles also have a lower scattering-to-attenuation ratio (STAR), meaning that they mainly attenuate the ultrasound signal. This value represents the microbubbles efficiency to enhance visualization of the tissue [14].

Larger microbubbles therefore seem more suitable as they last longer, allowing enough time for imaging, and are better scatterer. There are however additional risks with large microbubbles, as they could for example get trapped in the capillary vasculature, thus placing the restrictions on the microbubbles diameter to be smaller than  $8\mu\text{m}$  [15], corresponding to the average size of red blood cells.

### *Shell*

Due to the effect of surface tension, free gas microbubbles are inherently unstable and thus require a stabilizing shell to persist long enough in the bloodstream to be imaged.

The first microbubble shells were made of protein, more specifically albumin-coated shells [16]. Albumin improved the stability of the microbubbles by forming a thin shell that is relatively rigid.

Another composition that is used for a number of commercially available ultrasound contrast agent is lipid. The shell is composed of a lipid monolayer, which has two interesting characteristics: the low surface tension increases the stability of the microbubbles, while the high cohesiveness of the monolayer creates a shell that is resistant to shear deformation [16].

Finally, polymer-based shells are another commonly used composition. The shells made of polymer are generally thick and formed by cross-linked polymer chains and can be fabricated using a wide range of polymer species, allowing for some versatility in their production [16]. Polymer shells are very stable on the expense of reduced echogenicity.

### *Core*

One of the main problems with early contrast agents, namely air-filled microbubbles, was their low stability, resulting in the microbubbles dissolving very quickly, in about 10 ms, into the blood.

Nowadays, microbubbles are most commonly filled with perfluorocarbon gases. Due to their low solubility and diffusivity, contrast agents remain stable much longer than air-filled microbubbles, and have a relatively low toxicity [2].

## A.1.2. Oscillation modes

When an ultrasound wave insonates a gas-filled microbubble, the bubble begins to oscillate, meaning that it undergoes alternate phases of expansion and compression [17].

The microbubbles have different oscillation behaviors, depending on a number of parameters. Several models exist to model these behaviors, and include parameters such as microbubbles radius, shell stiffness, shell thickness, to only name a few [17]. Most importantly though, the acoustic pressure to which microbubbles are exposed directly influence their behavior. Three distinct behaviors can consequently be identified, based on the acoustic pressure range.

### *Linear behavior*

At low acoustic pressure (up to 20 kPa [18]), the microbubbles oscillate linearly, meaning that they oscillate in synchrony with the incident ultrasound wave. They expand during the negative part of the wave's cycle and compress during the positive part (Figure 17).

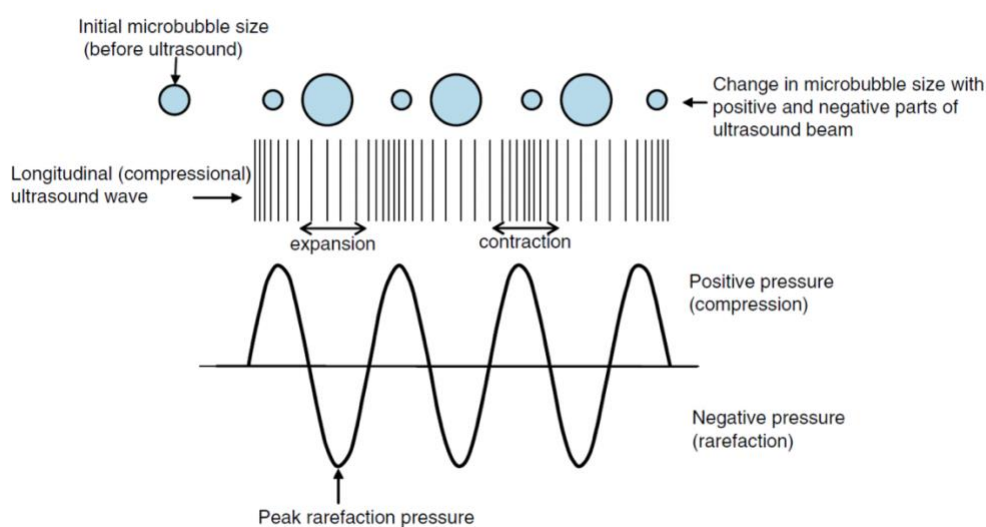


Figure 17: Microbubble changes in size with varying acoustic pressures [11]

The frequency of the backscattered signal from the microbubble is the same than the frequency of the incident ultrasound wave. Optimal scattering is obtained by matching the transmit frequency to the microbubble's resonance frequency, which is the frequency at which it oscillates most easily.

### *Non-linear behavior*

As the acoustic pressure increases (but commonly under  $\sim 1$  MPa [18]), the microbubble oscillations become asynchronous to the incident wave. Due to the solid structure of the shell and the gas present in the microbubble, it cannot contract infinitely, and thus means that under higher acoustic pressures, the microbubble expands more than it contracts. These non-linear oscillations result in a different backscattered signal, with non-linear components. The signal will contain the incident wave frequency (the fundamental frequency) but also harmonics, which are multiples of the fundamental frequency. The second harmonic (twice the fundamental frequency) usually has the strongest response intensity of all harmonics [19].

### *Destructive behavior*

When the acoustic pressure reaches values above 1 MPa, the strength of the oscillations will eventually cause the microbubble to rupture and release its gas core. The gas released will produced a strong transient echo with a wide range of non-linear components (Figure 18), but will also dissolve into the surrounding fluid, meaning that this backscattered signal rapidly disappears.

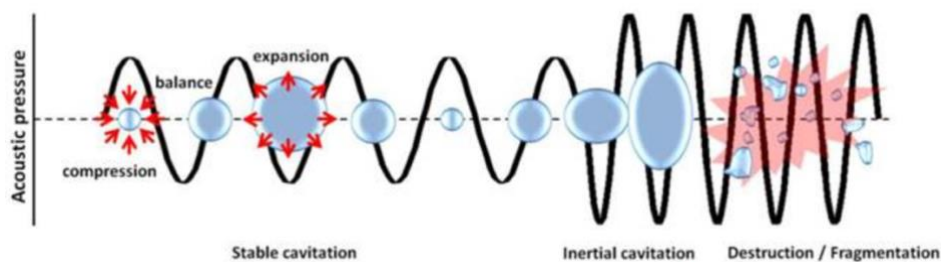


Figure 18: Microbubble response to increasing acoustic pressure [20]

## A.2. Imaging techniques

### A.2.1. Conventional imaging

Initially, only conventional imaging techniques were available to image ultrasound contrast agents. Those technique nonetheless allowed to obtain a contrast enhanced image since, as we have previously discussed, the backscattered signal contain a linear component of the same frequency that the one of the incident ultrasound wave [11].

#### *B-mode imaging*

In B-mode imaging, the image is constructed from the echoes formed by the ultrasound wave reflection and scattering. The increased backscattered signal from microbubbles injected into liquid cavities or blood vessels thus allows to increase the echogenicity of cavity or vessel in question, and in turn the opacity of the structure on the image generated.

The use of microbubbles in echocardiography for example, allowed a better visualization and delineation of the heart chambers, due to the number of microbubbles transiently accumulating in the left ventricle [21]. The technique then allowed physicians to more precisely estimate ventricular volumes and outputs.

The doses of contrast agents required to obtain such results, in the order of milliliters, were however much higher than doses nowadays used [11]. Very high concentrations also cause attenuation, which in turn cause shadowing of the deeper tissues, a trade-off is therefore needed to obtain an acceptable scattering-to-attenuation ratio [21].

Furthermore, the backscattered signal from surrounding tissues was still much stronger than that from the microbubbles. Strong acoustic pressure had to be applied to detect a significant enough signal, which resulted in destruction of the microbubbles. This means that the stronger echo from the collapsing microbubbles would only be transient and that microbubbles would need to continuously be replenished [21]. For these reasons, the benefit from ultrasound contrast agents remains limited with fundamental B-mode imaging.

#### *Doppler imaging*

While blood cells do not typically generate any significant echo, it has been observed that backscattered echoes are generated from microbubbles. For this reason, ultrasound contrast agents also proved beneficial for Doppler imaging techniques such as spectral Doppler, where the microbubbles are used to measure blood flow [19].

In the presence of microbubbles, the strength of the backscattered echoes from the blood are in fact increased by 20 to 30 dB [22]. This increase thus allows to measure blood flow in deeper blood vessels than when imaging without contrast agents.

Similarly, the enhanced strength of the backscattered signals from contrast agents is advantageous for color flow imaging techniques such as Color Doppler, in which the mean

frequency of each pixel is color-coded with red representing blood flowing towards the transducer and blue away from the transducer, and Power Doppler, in which the power of the backscattered signal is represented on a color scale (typically ranging through black, red, orange and yellow) [11].

The increased strength of the Doppler signal is in both cases helpful to better discriminate blood signal from clutter signal and noise.

There are however some drawbacks with the use of contrast agents with both techniques. With Color Doppler, the likelihood of seeing blooming artefacts is greater with contrast agents. Blooming corresponds to the color spreading beyond the walls of the vessel, thus making it look larger than it is. This is caused by the oversensitivity of the microbubbles, which are then producing echoes even when the central part of the ultrasound pulse is outside of the vessel [21].

Blooming artefacts deteriorate the spatial resolution of the image and can obscure the tissues surrounding the vessel.

Power Doppler is, on the other hand, less sensitive to blooming artefacts but suffers from low framerate. Combined with the slow replenishment of microbubbles in small vessels where the blood flow is slower, the technique does not perform well at visualizing small vessels in organs such as the heart or the liver [21].

### A.2.2. Contrast specific/Non-linear imaging

Although conventional imaging techniques benefit from the use of ultrasound contrast agents, the enhancement provided by the strong backscattering power of microbubbles is not enough to visualize deeper tissues or small vessels with such techniques.

Contrast specific techniques have therefore been developed to take advantage of the non-linear behavior of microbubbles within certain ultrasound fields.

Microbubbles behavior varies with the acoustic pressure they are exposed to. The amplitude of the transmitted pulses can be controlled by the ultrasound operator with the transmit power control of the imaging system. The transmitted acoustic pressure is however not shown on the system display, and the changes in transmit power are reflected by the Mechanical Index value displayed on the screen [11].

The mechanical index (MI) is an index formulated to “quantify the likelihood of onset of inertial cavitation” [11], which corresponds to microbubbles exhibiting a destructive behavior. Hence, a high MI indicates high acoustic pressure. It is defined as:

$$MI = \frac{p_r}{\sqrt{f}}$$

With  $p_r$  the peak rarefaction pressure (or peak negative pressure) in MPa and  $f$  the frequency of the ultrasound wave in MHz [11].

Contrast-specific imaging technique are commonly divided in two main categories [11].

Low-MI techniques are techniques where the acoustic pressure used elicits non-linear behavior in the exposed microbubbles, whereas high-MI techniques use higher acoustic pressures causing the microbubbles to behave in a destructive manner.

#### *Low-MI techniques*

The aim of low-MI techniques is to detect the non-linear components, or harmonics, of the backscattered signal from the microbubbles. Most often, the second harmonic is chosen, as it usually has the highest intensity of all harmonics generated and because the frequency bandwidth of currently available array transducers is often limited to 70-80% of the center frequency and thus limits higher harmonic imaging.

The techniques can detect the harmonic by processing the differences between the backscattered signals obtained from two or more transmitted pulses. Pulse inversion with two transmissions, pulse inversion with three transmissions, amplitude modulation (also

called power modulation), binary coding, or chirp coding are a few examples of such low-MI techniques [21].

The current study focuses on pulse inversion with two transmissions. In this technique, two consecutive pulses are transmitted, with the waveform of the second pulse being inverted compared to the first one. The two received echoes are then stored and added together. Under low MI, where the microbubbles oscillate in the linear regime, the response to positive and negative pressures is therefore similar, meaning that the linear components of the second echo will be cancelled out by the linear components of the first echo.

At higher pressure, or MI, where they oscillate in the non-linear regime, microbubbles respond differently to positive and negative pressures (as we mentioned before, they expand more than they contract). The non-linear components of the backscattered echoes from the microbubbles for both signals will therefore not cancel each other out and constitute the resulting signal (Figure 19).

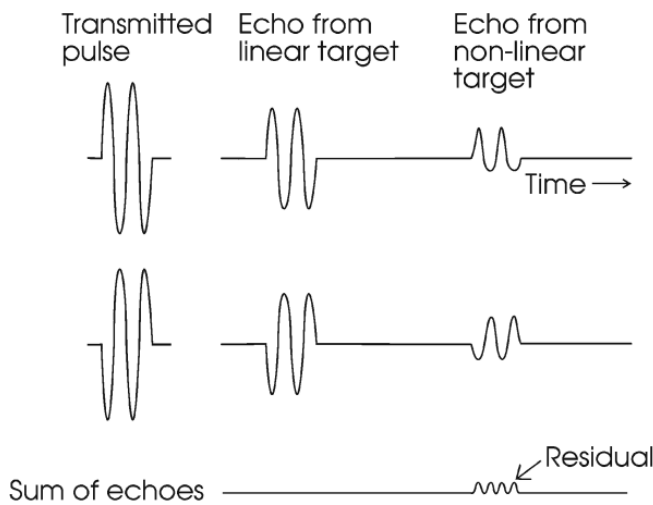


Figure 19: Illustration of the pulse inversion imaging technique [21]

### High-MI techniques

With high-MI techniques, a better sensitivity can be achieved by using pulse amplitudes that are high enough to destruct the microbubbles. When the microbubbles collapse, they release the gas they contained, which produces a strong backscattered signal.

By combining low-MI techniques to visualize the microbubbles before and/or after applying the destructive pulse sequence, perfusion of, for example, the myocardium can be measured [11].

Since the contrast-enhanced images are obtained using the echo from the collapsing microbubbles, only intermittent acquisition can be performed. Frame by frame images are recorded and the microbubbles distribution can be measured by reviewing the recording [21].

## A.3. Acoustic droplet vaporization

While ultrasound contrast agents in the form of microbubbles have been used in diagnostic and therapeutic applications, to enhance the sensitivity of ultrasound imaging, in targeted drug delivery or for blood clot fragmentation to name a few [2], their relatively large size (in the order of microns) prevents their entry into the extravascular space and accelerates their clearance from the circulation [3]. These factors thus create limitations to the applications of microbubbles as theranostic agents.

In the 1990s, a phenomenon called Acoustic Droplet Vaporization (ADV) was first described and provided a promising solution to these issues. ADV, in which liquefied nanoparticles or droplets undergo a phase change from liquid to gas as a result of the application of acoustic waves [3], takes advantage of the vapor pressure of a liquid, which is connected to the temperature.

By controlling when the phase shift of the droplets occurs, the nanometer-sized droplets can be delivered to a specific target site, for instance in tumor capillaries or at some extravascular site, as represented in Figure 20.

Their small size also greatly reduces their rate of clearance from the circulation.

Once the droplets have transitioned to gas microbubbles, the qualities of microbubbles, such as their increased echogenicity or their potential for targeted drug delivery, can then be exploited.

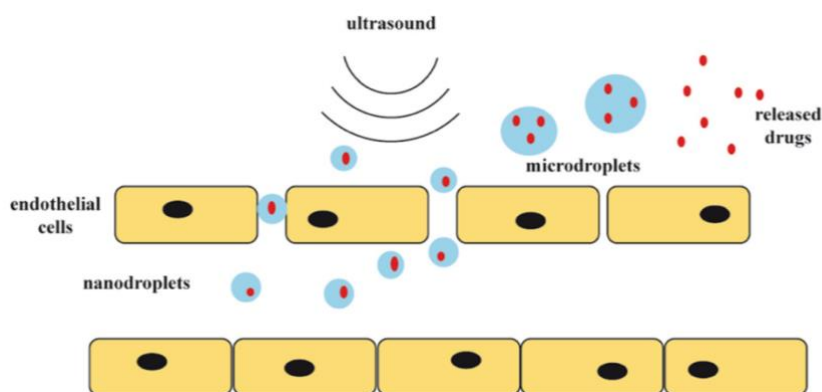


Figure 20: Illustration showing the extravasation of nanodroplets through endothelial cell gaps [2]

### A.3.1. Vaporization

As mentioned before, ADV is based on the vapor pressure of a liquid, which can be defined as “the pressure of the specified gas in equilibrium with its own liquid in a closed system at a specified temperature” [2]. The vapor pressure of a liquid increases as its temperature does, and its boiling point is defined as the temperature at which the vapor pressure is exactly 1 atm pressure [3]. At this temperature and above, a gas phase can form, and the liquid can boil to gas.

Even at a temperature above their boiling point though, liquids can remain in their liquid state, because a nucleation event is first needed to initiate the formation of a gas phase, which is generally difficult to create. Liquids in this state are said to be in a “superheated state” [3].

In an appropriate acoustic field, nucleation events are likely to occur during the negative part of the ultrasonic wave, when the pressure within the droplet is below the vapor pressure of the liquid. As the amplitude of the peak negative pressure of the ultrasonic wave increases (Figure 21), the probability of nucleation events, and as a consequence of droplet vaporization, increases [2].

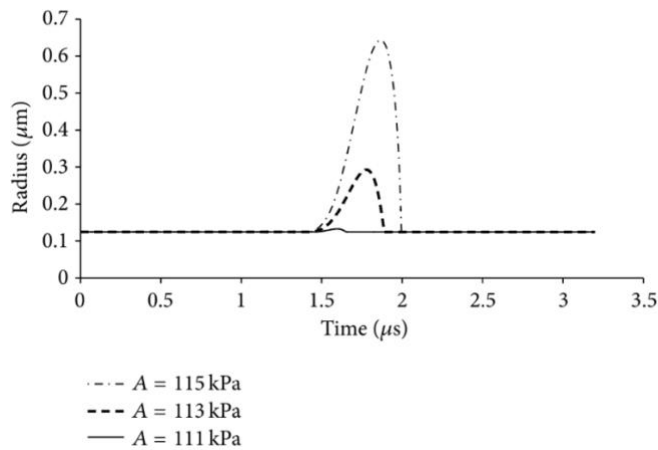


Figure 21: Radius of an expanding bubble as a function of time and acoustic amplitude [3]

Therefore, to achieve ADV, liquid with a boiling point near or below body temperature should be chosen and exposed to an acoustic field favorable to acoustic cavitation.

### A.3.2. Droplet structure and composition

Similarly to gas microbubbles, nanoparticles must have certain important properties to be used in ADV. These includes a long circulation time, biocompatibility, non- or acceptable toxicity but also compatibility with commercially available ultrasound imaging systems [2].

#### *Biocompatibility and toxicity*

Because the applications of ADV we are discussing here are medical applications, it is crucial that the liquid used is biocompatible and non-toxic. With their relatively low toxicity, perfluorocarbons are well-suited for such use [2].

However, the surfactants used for the stabilizing shell should also be considered. Lipid-based (phospholipids) and protein-based (human proteins) are stabilizing agents that have been used and known to be non-toxic, whereas non-toxicity remains to be proven for a number of synthetic polymers [3].

#### *Stability*

Perfluorocarbons also are good candidates for ADV due to their low solubility and diffusivity in water-based liquids. This means that the lifetime of perfluorocarbon droplets is considerably higher than that of microbubbles (in the order of several days) but also that perfluorocarbon gas-filled microbubbles remain stable for a much longer period than air-filled microbubbles of the same size [2].

### A.3.3. Applications

Ultrasound has been, for many years now, a valuable diagnostic tool with many advantages, such as low cost, safety, temporal resolution, to only name a few.

The technique has also suffered from a number of limitations, and many additional techniques have since been developed to overcome them.

ADV is one of them and has many different applications, both in the diagnostic and therapeutic fields. Our aim here is to present a few of them.

### *Diagnostic applications*

- Vascular imaging

The main purpose of ultrasound contrast agents has largely been to improve the sensitivity of the imaging technique by increasing the strength of the received signal.

Although relatively large microbubbles are necessary to generate a strong enough backscattered signal, in comparison to the signal from the surrounding tissue, too large microbubbles cannot traverse the lungs and thus recirculate and are not able to reach certain vessels due to their elevated clearance rate. Droplets and ADV offer a solution to these issues and now allows contrast-enhanced imaging of regions that could previously not be reached by regular contrast agents [3].

- Cancer detection

Tumor imaging is critical for early cancer detection, but micron-sized contrast agents are unfortunately unable to penetrate the endothelial barrier and reach the tumor vasculature.

The engineering of nanodroplets with specific ligands to cancerous cells provides a possibility to detect tumors, either by binding of the droplets to the tumor cells, or by visualizing and characterizing the vasculature of the suspected area [3].

### *Theranostic/Therapeutic applications*

- Drug delivery

It is especially important for some drug delivery techniques to be as accurately localized as possible, as to avoid negative effects on healthy tissues. This for example applies to drug delivery in tumor therapy.

Nanodroplets, as mentioned before, can be used to reach the target site, the tumor in that case. These droplets, loaded with therapeutic agents, can first be vaporized into microbubbles and used as contrast agents to localize and confirm the site of delivery. Then, by exposing them to a high acoustic pressure, the microbubbles can be disrupted, and their shell ruptured, thus releasing their content, which includes the therapeutic agents [2].

- Embolotherapy

A different method to treat tumors than drug therapy is to starve the tumor by reducing their blood supply. This can be achieved by occluding the vessels feeding them with gas bubbles [2].

As the droplets flow through the targeted vessels, they are vaporized at a chosen location using a focused ultrasound beam. The gas bubbles created then occlude the blood flow downstream from this point and damage the tumor [3].

Although the technique shows a great potential for clinical use, embolotherapy with ADV should be carefully considered as arterial emboli can create infarcts in the heart or the brain [2].

## **A.4. Limitations**

Although they show great promises, the majority of current ADV techniques still are at the preclinical study stage, which means more research needs to be done to ensure their safety and efficacy [3].

As for any medical application, safety is an essential requirement. The perfluorocarbons used in the fabrication of droplets are generally considered to be non-toxic, but as mentioned before, the surfactants used to stabilize the droplets also need to be assessed. Non-toxicity of synthetic polymers has for example not yet been proven [3]. On the other

hand, surfactants such as natural phospholipids, polysaccharides and human proteins are considered to be the safest agents to use [2].

Another aspect of safety to be considered is physical safety. Premature vaporization of the droplets could be problematic and cause adverse effects, such as endothelial damage [3]. It is therefore crucial to fully understand how and when droplets convert into microbubbles.

Finally, clearance rates of the droplets in the body also are a safety concern. One advantage of nanodroplets over microbubbles for therapeutic applications is their reduced clearance rate, due to their smaller size, but it is also important to ensure that circulating droplets do not cause short- or long-term effects, and that they can be eliminated by the body [2].

A direct result of the principles of ultrasound propagation in tissue, some fundamental limitations of ultrasound itself should lastly be mentioned. Such a limitation is encountered when the ultrasound wave travels through soft tissue and meets a gas-filled structure, such as the lungs, the stomach or gas pockets in the intestines. Since more than 99% of the wave is reflected at a soft tissue-air interface [11], no useful echoes can be obtained beyond this point.

Similarly, it is difficult to obtain useful echoes from structures behind bones, as about 50% of the ultrasound wave is reflected at interfaces between soft tissue and bone [11],

This thus limits the structures and organs that can be reached by an ultrasound wave, both for diagnostic and therapeutic purposes.

Increasingly common too, the attenuation of ultrasound on overweight and obese patients, caused by the low speed of sound in fat [11], makes it difficult or even impossible to target structures otherwise accessible on patients with lower body mass index (BMI).

## References

- [1] Sophie Hernot, Alexander L. Klibanov. Microbubbles in ultrasound-triggered drug and gene delivery. *Advanced Drug Delivery Reviews*, Volume 60, Issue 10, 2008.
- [2] Yufeng Zhou. Application of acoustic droplet vaporization in ultrasound therapy. *Journal of Therapeutic Ultrasound*, 2015.  
(<http://creativecommons.org/licenses/by/4.0/>)
- [3] Chung-Yin Lin and William G. Pitt. Acoustic droplet vaporization in biology and medicine. *BioMed Res. Int.*, 2013.
- [4] Connor Puett, Paul S. Sheeran, Juan D. Rojas, Paul A. Dayton. Pulse sequences for uniform perfluorocarbon droplet vaporization and ultrasound imaging. *Ultrasonics*, Volume 54, Issue 7, 2014.
- [5] Ron Daigle. Verasonics Sequence Programming Tutorial. 2012.
- [6] ATS Laboratories. Peripheral Vascular Doppler Flow Phantom, Models ATS 524 & 525. Available: <http://www.atslaboratories-phantoms.com/resources/Model-524-525-Data-Sheet.pdf> (accessed March 2019).
- [7] Jonna Ojala, Miikka Visanko, Ossi Laitinen, Monika Österberg, Juho Antti Sirviö, Henrikki Liimatainen. Emulsion Stabilization with Functionalized Cellulose Nanoparticles Fabricated Using Deep Eutectic Solvents. *Molecules*. 2018.
- [8] Morteza Ghorbani, Karl Olofsson, Anna Justina Svagan, Dmitry Grishenkov. Unravelling the Acoustic and Thermal Responses of Pickering Emulsions Stabilized with Cellulose Nanofibers. Submitted to *Langmuir*. Under Revision.
- [9] Ron Daigle. Verasonics Sequence Programming Manual. 2012.
- [10] Lisa Brannon-Peppas, James O. Blanchette. Nanoparticle and targeted systems for cancer therapy. *Advanced Drug Delivery Reviews*, Volume 64, Supplement, 2012.
- [11] Peter R. Hoskins, Kevin Martin, Abigail Thrush. *Diagnostic ultrasound: physics and equipment*. Cambridge University Press, 2010.
- [12] Fabrizio Calliada, Rodolfo Campani, Olivia Bottinelli, Anna Bozzini, Maria Grazia Sommaruga. Ultrasound contrast agents: Basic principles. *European Journal of Radiology*, Volume 27, Supplement 2, 1998.
- [13] Ajit Raisinghani, Anthony N. DeMaria. Physical principles of microbubble ultrasound contrast agents. *The American Journal of Cardiology*, Volume 90, Issue 10, Supplement 1, 2002.
- [14] Shashank Sirsi, Jameel Feshitan, James Kwan, Shunichi Homma, Mark Borden. Effect of Microbubble Size on Fundamental Mode High Frequency Ultrasound Imaging in Mice. *Ultrasound in Medicine & Biology*, Volume 36, Issue 6, 2010.
- [15] M. Schneider. SonoVue, a new ultrasound contrast agent. *Eur. Radiol.* 9 (Suppl. 3), 1999.

- [16] Shashank Sirsi, Mark Borden. Microbubble Compositions, Properties and Biomedical Applications. Bubble science engineering and technology, Volume 1, 2009.
- [17] Michiel Postema, Annemieke van Wamel, Charles T. Lancée, Nico de Jong. Ultrasound-induced encapsulated microbubble phenomena. Ultrasound in Medicine & Biology, Volume 30, Issue 6, 2004.
- [18] Nico De Jong, Marcia Emmer, Chien Ting Chin, Ayache Bouakaz, Frits Mastik, Detlef Lohse, Michel Versluis. "Compression-Only" Behavior of Phospholipid-Coated Contrast Bubbles. Ultrasound in Medicine & Biology, Volume 33, Issue 4, 2007.
- [19] Jean-Michel Correas, Lori Bridal, Amélie Lesavre, Arnaud Méjean, Michel Claudon, Olivier Hélénon. Ultrasound contrast agents: properties, principles of action, tolerance, and artifacts. European Radiology, 2001.
- [20] Hao-Li Liu, Ching-Hsiang Fan, Chien-Yu Ting, Chih-Kuang Yeh. Combining Microbubbles and Ultrasound for Drug Delivery to Brain Tumors: Current Progress and Overview. Theranostics, 2014.
- [21] Thomas A. Whittingham. Contrast-Specific Imaging Techniques: Technical Perspective. In: Contrast Media in Ultrasonography, Medical Radiology (Diagnostic Imaging), 2005.
- [22] Katherine W. Ferrara, Christopher R.B. Merritt, Peter N. Burns, F. Stuart Foster, Robert F. Mattrey, Samuel A. Wickline. Evaluation of tumor angiogenesis with US: Imaging, Doppler, and contrast agents. Academic Radiology, Volume 7, Issue 10, 2000.



TRITA CBH-GRU-2019:084